https://doi.org/10.15407/ujpe65.5.400

A.K. SHUAIBOV, A.I. MINYA, A.A. MALININA, R.V. GRITSAK, A.N. MALININ

Uzhgorod National University

(3, Narodna Sq., Uzhgorod 88000, Ukraine; e-mail: alexsander.shuaibov@uzhnu.edu.ua)

CHARACTERISTICS OF THE NANOSECOND OVERVOLTAGE DISCHARGE BETWEEN $CuInSe_2$ CHALCOPYRITE ELECTRODES IN OXYGEN-FREE GAS MEDIA

The characteristics of the nanosecond overvoltage discharge ignited between semiconductor electrodes based on the $CuInSe_2$ chalcopyrite compound in the argon and nitrogen atmospheres at gas pressures of 5.3–101 kPa are reported. Due to the electrode sputtering, chalcopyrite vapor enters the discharge plasma, so that some $CuInSe_2$ molecules become destroyed, whereas the others become partially deposited in the form of thin films on solid dielectric substrates located near the plasma electrode system. The main products of the chalcopyrite molecule decomposition in the nanosecond overvoltage discharge are determined; these are atoms and singly charged ions of copper and indium in the excited and ionized states. Spectral lines emitted by copper and indium atoms and ions are proposed, which can be used to control the deposition of thin chalcopyrite films in the real-time mode. By numerically solving the Boltzmann kinetic equation for the electron energy distribution function, the electron temperature and density in the discharge, the specific losses of a discharge power for the main electronic processes, and the rate constants of electronic processes, as well as their dependences on the parameter E/N, are calculated for the plasma of vapor-gas mixtures on the basis of nitrogen and chalcopyrite. Thin chalcopyrite films that effectively absorb light in a wide spectral interval (200–800 nm) are synthesized on quartz substrates, by using the gas-discharge method, which opens new prospects for their application in photovoltaic devices.

Keywords: nanosecond overvoltage discharge, argon, nitrogen, chalcopyrite, plasma.

1. Introduction

Thin $CuInSe_2$ chalcopyrite films are widely used in various photovoltaic devices [1]. However, the production of those films with the use of physical methods is mainly based on the laser sputtering method, at which the stoichiometric composition of the film remains the same as in the massive laser target. This method of synthesis of chalcopyrite films is rather expensive because of a high cost of the laser and vacuum technologies. In adition, it has technological limitations at the synthesis of thin films with large areas. Therefore, cheaper physical methods to synthesize thin chalcopyrite films may be promising, e.g., by sputtering massive electrodes in a strong electric field created by a nanosecond overvoltage discharge excited in gases at the atmospheric pressure.

In particular, in works [2, 3], we reported the results of our study concerning the parameters of a plasma based on the $CuInSe_2$ compound in air at the atmospheric-pressure, when chalcopyrite electrodes were sputtered in the nanosecond overvoltage discharge. The presence of oxygen in this plasma can stimulate the synthesis of nanostructures from cop-

per or indium oxides [4], the influence of which on the properties of chalcopyrite films has been poorly investigated. Therefore, a challenging task is the study of the chalcopyrite electrode sputtering in oxygen-free gaseous media (N_2, Ar) and the characteristics of such plasma in the close connection with the parameters of synthesized chalcopyrite films.

Nanosecond and sub-nanosecond atmospheric-pressure discharges can be rather homogeneous, which makes them suitable for the thin film deposition onto solid dielectric substrates. However, the characteristics of such discharges have been most extensively studied only for metal electrodes separated by distances of 0.01–0.15 m and in the case of discharge excitation with the help of unique high voltage pulse generators of sub-nanosecond pulses 100–250 kV in amplitude [5, 6]. Less studied are nanosecond discharges ignited between semiconductor electrodes under the condition of strong overvoltage across the discharge gap, when the electrode distance falls within an interval of $(1\div3)\times10^{-3}$ m, and the electrode system provides a moderate inhomogeneity of the electric field strength distribution.

This paper presents the results of our research of the radiation emitted by the plasma of vapor-gas mixtures N_2(Ar)–$CuInSe_2$ in a nanosecond overvoltage discharge at the atmospheric-pressure with the injection of the material of a pair of chalcopyrite-based electrodes into the gas medium by means of the electrode sputtering. We also studied the spectra of the plasma radiation transmitted through the synthesized chalcopyrite films within a wavelength interval 200–800 nm. The results of simulations for the parameters of plasma on the basis of the mixture of atmospheric-pressure nitrogen and copper vapor are also presented.

2. Experimental Equipment and Conditions

A high-current nanosecond discharge between chalcopyrite ($CuInSe_2$) electrodes was excited in a hermetically sealed plexiglas discharge chamber (Fig. 1). The interelectrode distance was 10^{-3} m. The chamber with the electrode system was evacuated with the help of a vacuum pump to a residual air pressure of 10 Pa. Then, high purity nitrogen or argon was inlet into the chamber, so that the buffer gas pressure was within an interval 5–101 kPa. The diameter of cylindrical electrodes was 5×10^{-3} m. The curvature radii of the working end faces of semiconductor electrodes were identical and equal to 3×10^{-3} m.

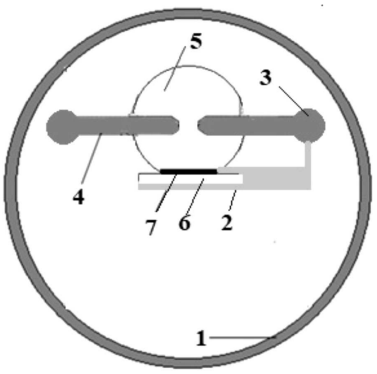

Fig. 1. Schematic diagram of gas-discharge module: hermetic case of discharge chamber (*1*), fastening of the substrate for sputtering (*2*), system to control the distance between the electrodes (*3*), chalcopyrite electrodes (*4*), gas region, where the sputtering occurs (*5*), glass or quartz substrate for thin-film sputtering (*6*), layer of sputtered substance on the basis of electrode material (*7*)

The high-current nanosecond discharge was ignited with the help of a bipolar high-voltage pulse modulator generating pulses 50–150 ns in duration and 40–60 kV in amplitude for positive and negative components. The repetition frequency of voltage pulses, f, could be varied from 40 to 1000 Hz, but the main researches were performed at a frequency of 100 Hz. The oscillograms of voltage pulses across the discharge gap and the oscillograms of current pulses were registered by means of a wide-band capacitive voltage divider, a Rogowski coil, and a wide-band 6LOR-04 oscilloscope. The time resolution of this system for measuring the characteristics of electrical pulses was 2–3 ns.

To register the radiation spectra of the nanosecond overvoltage discharge, an MDR-2 monochromator and an FEU-106 photomultiplier were applied. A signal from the photomultiplier was supplied to the amplifier and registered on a personal computer display with the help of an amplitude-to-digital converter in an automated spectral measurement system. The discharge radiation was analyzed in a spectral interval 200–650 nm. The experimental method and equipment were described in works [2, 4] in more details.

When a quartz or glass substrate was mounted at a distance of 3×10^{-2} m from the discharge gap center

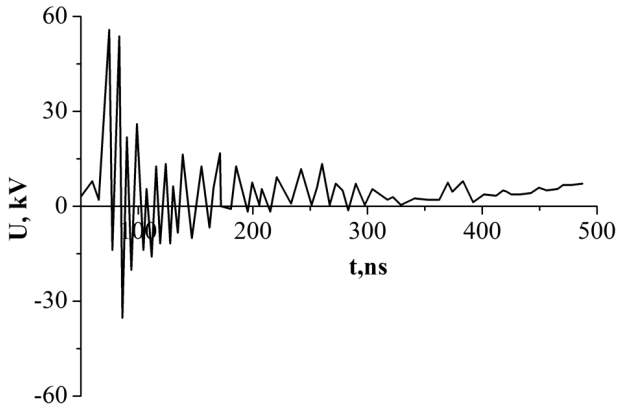

Fig. 2. Oscillograms of the current (up) and voltage (down) pulses between electrodes on the basis of $CuInSe_2$ compound at a nitrogen pressure of 5.3 kPa in the discharge chamber

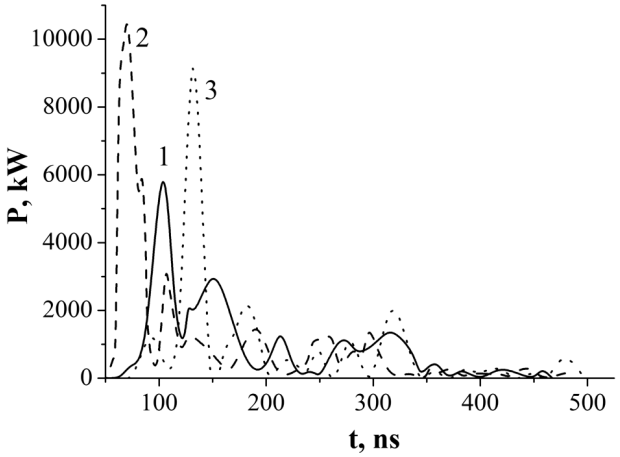

Fig. 3. Pulse power of nanosecond overvoltage discharge at $p(\mathrm{Ar})$ = 101 kPa (*1*), $p(\mathrm{Ar})$ = 202 kPa (*2*), and $p(N_2)$ = = 202 kPa (*3*)

(Fig. 1) and after the discharge (with f = 100 Hz) burned for 2–3 h, the deposition of a gray film from the products of the electrode sputtering onto the substrate was observed. The obtained film specimens were analyzed by means of transmitting light through them in a wide radiation spectral interval deuterium and incandescent lamps (200–850 nm). The corresponding experiments were performed, by using a spectral complex created on the basis of an MDR-23 monochromator, at room temperature, and according to the procedure described in work [7].

A nanosecond overvoltage discharge was ignited in the system of chalcopyrite electrodes of the "sphere-sphere" type with the inter-electrode distance d = $= 10^{-3}$ m and in the nitrogen or argon atmosphere with pressures varied from 5 to 202 kPa. The discharge had a diffusive spherical form, although it was ignited making no use of a separate pre-ionization system. For the discharges of this type, the role of a preionization system can be played by an electron beam or an X-ray one [5]. At low gas pressures (1–10 kPa), a threshold can be reached, when most of plasma electrons transit into a continuous acceleration mode [8]. However, the electron escape efficiency at atmospheric gas pressures decreases drastically. Therefore, the most probable mechanism of discharge gap preionization is by means of X-ray radiation.

The discharge volume depended on the repetition frequency of voltage pulses. The discharge emitter operated in the "point lamp" mode only at low values of this parameter (f = 40÷150 Hz). When the repetition frequency grew from 40 to 1000 Hz, the plasma volume in the discharge emitter increased from 1 to 100 mm^3. A characteristic oscillogram of the voltage across the discharge gap and the electrical pulse power of a nanosecond overvoltage discharge are shown in Figs. 2 and 3. Figure 3 demonstrates the discharge pulse power at a high pressure of gas mixtures, which could reach a value of 202 kPa, but the optical characteristics of plasma at a pressure of 202 kPa were not studied. In the experiment, we observed voltage oscillations across the discharge gap with a half-period close to 10 ns, which were induced by a mismatch between the output impedance of a high-voltage pulse modulator and the load. At a nitrogen pressure of 5.3 kPa, the maximum amplitude of the voltage peaks fell within an interval 40–55 kV. But when the nitrogen pressure was increased to 101 kPa, the amplitude of voltage pulses with the positive and negative polarities decreased to 40 kV [9].

The pulses of a discharge current looked like damping oscillations with amplitudes up to 150 A. The main fraction of the electric pulse power was introduced into the plasma of a nanosecond overvoltage discharge within the first 100–150 ns. The maximum pulsed electric discharge power in the argon–$CuInSe_2$ mixture was attained at $p(\mathrm{Ar})$ = 202 kPa and was equal to 10.5 MW. In the case of argon at the atmospheric-pressure, it decreased approximately twice (Fig. 3). The highest pulse power in the nitrogen-based mixtures was achieved at $p(N_2)$ = = 202 kPa and was equal to 9 MW (Fig. 3), whereas it decreased to 7 MW at $p(N_2)$ = 101 kPa.

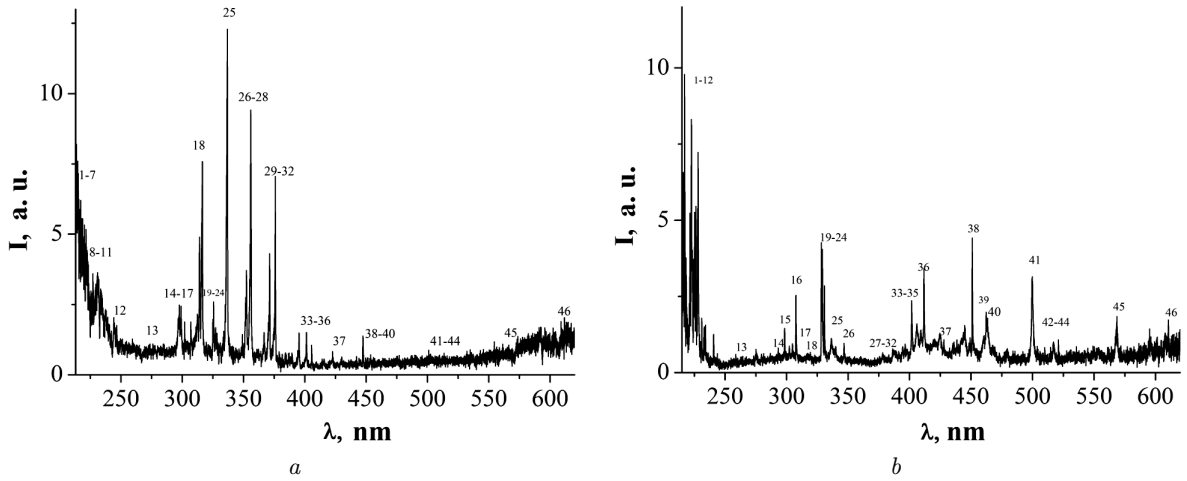

a *b*

Fig. 4. Radiation emission spectra of nanosecond overvoltage discharge plasma at nitrogen pressures of 5.3 (*a*) and 101 kPa (*b*)

The graphical integration of the pulse power over the time made it possible to determine the energy introduced into the plasma during one discharge pulse. In particular, the energy contribution to the plasma from the discharge in the nitrogen-based vapor-gas mixtures fell within an interval 350–375 mJ. The energy contribution to the plasma by one pulse in the case of argon-based vapor-gas mixtures was equal to 400 mJ at $p(\mathrm{Ar}) = 101$ kPa and increased to 440 mJ at $p(\mathrm{Ar}) = 202$ kPa.

3. Optical Characteristics of Plasma

Figure 4 illustrates the emission spectra of nanosecond overvoltage discharges excited between the electrodes on the basis of $CuInSe_2$ compound at nitrogen pressures of 5.3 and 101 kPa. Table 1 demonstrates the results of identification of the most intense spectral lines and molecular bands in the emission spectra of a discharge plasma exhibited in Fig. 4.

The spectral lines of atoms and ions are observed against a continuous background of plasma radiation, which may be associated with the thermal radiation of plasma or with the plasma recombination radiation. As was shown in work [10], the copper and indium atoms are least strongly bound in the chalcopyrite molecules composing the massive electrodes. Therefore, the linear component of the plasma radiation spectrum is predominantly associated with separate spectral lines of atoms and singly charged ions of copper and indium both in the case of laser plasma formed at the target surface under vacuum conditions [11, 12] and in the case of atmospheric-pressure gas-discharge plasma [13].

The radiation emission spectrum of the gas component mostly manifested itself at low nitrogen pressures. It mainly consisted of intense bands in the spectral interval 280–390 nm belonging to the second positive system of a nitrogen molecule. At a low nitrogen pressure ($p = 5.3$ kPa), the radiation spectrum of the nanosecond overvoltage discharge plasma in the wavelength interval 200–230 nm included a group of closely located spectral lines belonging to a copper atom and a singly charged copper ion, and low-intensity lines of a singly charged indium ion (spectral lines 1 to 13 in Table 1). The spectral lines of copper were similar to those detected in the emission spectra of the nanosecond overvoltage discharge in atmospheric-pressure air between copper electrodes located at the distance $d = 2 \times 10^{-3}$ m from each other [14, 15]. This group of spectral lines is obtained in the case of sputtering the electrodes fabricated on the basis of $CuInSe_2$ compound in the discharge of the same type in atmospheric-pressure air at $d = (1 \div 2) \times 10^{-3}$ m and has not been studied earlier [16].

A group of intense spectral lines and bands is also observed in a spectral interval 290–410 nm (lines and bands 14 to 35 in Table 1). The spectral lines of a copper atom (lines 16, 19–24, 26, and 33) and the intense bands of the second positive system of a nitrogen molecule (bands 14, 18, 25, 27–32, 34, and 35)

Table 1. **Identification of the most intense spectral lines and bands of the products of the chalcopyrite molecule decomposition in the overvoltage nanosecond discharge at $p(N_2) = 5.3$ and 101 kPa**

No.	λ, nm	I, rel. units (at $p(N_2) = 5.3$ kPa)	I, rel. units (at $p(N_2) = 101$ kPa)	Object	E_{low}, eV	E_{up}, eV	Lower term	Upper term
1	216.50	4.42	9.8	CuI	0.00	5.72	$4s\,^2S$	$4p'\,^2D^0$
2	218.17	5.13	3.76	CuI	0.00	5.68	$4s\,^2S$	$4p'\,^2P^0$
3	220.97	4.12	2.25	CuII	8.78	14.39	$4p\,^3D^0$	$4d\,^3D$
4	221.45	5.16	5.14	CuI	1.39	6.98	$4s^2\,^2D$	$4p''\,^2P^0$
5	222.56	4.35	8.31	CuI	0.00	5.57	$4s\,^2S$	$4p'\,^4D^0$
6	224.26	2.94	3.72	CuII	3.26	8.78	$4s\,^1D$	$4p\,^3D^0$
7	224.70	2.10	5.26	CuII	2.72	8.23	$4s\,^3D$	$4p\,^3P^0$
8	226.37	2.52	5.45	CuII	8.92	14.39	$4p\,^1F^0$	$4d\,^3D$
9	227.62	2.64	5.37	CuII	2.98	8.42	$4s\,^3D$	$4p\,^3P^0$
10	231.32	3.63	1.78	InII	12.10	17.46	$5s5d\,^1D$	$5s9p\,^1P^0$
11	233.45	2.87	1.50	InII	12.68	17.99	$5s5d\,^3D$	$5s8f\,^3F^0$
12	240.66	1.77	1.25	CuI	1.64	6.79	$4s^2\,^2D$	$6p\,^2P^0$
13	274.97	0.90	0.65	InII	12.10	16.61	$5s5d\,^1D$	$5s5f\,^1F^0$
14	297.68	2.47	0.62	N_2	Second positive system $C^3\Pi_u^+$–$B^3\Pi_g^+$ (2;0)			
15	298.63	2.43	1.45	CuII	14.20	18.35	$4d\,^3S$	$5f\,^1D^0$
16	307.38	3.98	2.53	CuI	1.39	5.42	$4s^2\,^2D$	$4p'\,^2F^0$
17	314.27	4.9	0.52	InII	12.66	16.60	$5s5d\,^3D$	$5s9f\,^3F^0$
18	15.93	7.6	0.46	N_2	Second positive system $C^3\Pi_u^+$–$B^3\Pi_g^+$ (1;0)			
19	324.75	1.97	0.50	CuI	0	3.82	$4s\,^2S$	$4p\,2P^0$
20	327.39	1.68	0.50	CuI	0	3.39	$4s\,^2S$	$4p\,^2P^0$
21	328.27	1.48	4.26	CuI	5.15	8.93	$4p'\,^4F^0$	$4d'\,^2G$
22	329.05	1.13	4.04	CuI	5.07	8.84	$4p'\,^4F^0$	$4d'\,^4F$
23	330.79	1.02	2.84	CuI	5.07	8.82	$4p'\,^4F^0$	$4d'\,^4G$
24	333.78	1.55	0.66	CuI	1.39	5.10	$4s^2\,^2D$	$4p'\,^4F^0$
25	337.13	12.3	0.85	N_2	Second positive system $C^3\Pi_u^+$–$B^3\Pi_g^+$ (0;0)			
26	348.37	1.29	0.41	CuI	5.51	9.06	$4p'\,^4D^0$	$4d'\,^4G$
27	350.05	2.63	0.45	N_2	Second positive system $C^3\Pi_u^+$–$B^3\Pi_g^+$ (2;3)			
28	357.69	9.41	0.36	N_2	Second positive system $C^3\Pi_u^+$–$B^3\Pi_g^+$ (0;1)			
29	367.19	1.50	0.33	N_2	Second positive system $C^3\Pi_u^+$–$B^3\Pi_g^+$ (3;5)			
30	371.05	4.30	0.40	N_2	Second positive system $C^3\Pi_u^+$–$B^3\Pi_g^+$ (2;4)			
31	375.54	7.0	0.53	N_2	Second positive system $C^3\Pi_u^+$–$B^3\Pi_g^+$ (1;3)			
32	394.30	1.45	0.82	N_2	Second positive system $C^3\Pi_u^+$–$B^3\Pi_g^+$ (2;5)			
33	402.26	1.50	2.36	CuI	3.79	6.87	$4p\,^2P^0$	$5d\,^2D$
34	405.94	1.04	1.6	N_2	Second positive system $C^3\Pi_u^+$–$B^3\Pi_g^+$ (0;3)			
35	409.48	0.45	1.4	N_2	Second positive system $C^3\Pi_u^+$–$B^3\Pi_g^+$ (4;8)			
36	410.17	0.36	3.42	InI	–	3.02	$5s^25p\,^2P^0$	$5s^26s\,^2S_{1/2}$
37	427.99	0.4	1.07	CuII	15.07	17.96	$5p\,^3D^0$	$7s\,^3D$
38	451.13	0.6	4.41	InI	0.27	3.02	$5s^25p\,^2P^0$	$5s^26s\,^2S_{1/2}$
39	459.97	0.54	1.13	N_2^+	$2^\Sigma \rightarrow 2^\Sigma$ (2;4)			
40	462.07	0.4	1.97	InII	15.33	18.01	$5s4f\,^3F^0$	$5s_{1/2f=4}8g$
41	500.52	0.52	3.08	NII	25.50	27.97	$3s\,^5P$	$3p\,^5P^0$
42	510.55	0.45	0.82	CuI	1.39	3.82	$4s^2\,^2D$	$4p\,^2P^0$
43	515.83	0.50	0.94	CuI	5.69	8.09	$4p'\,^2P^0$	$5s'\,^2D$
44	521.82	0.58	1.07	CuI	3.82	6.19	$4p\,^2P^0$	$4d\,^2D$
45	570.02	0.58	1.27	CuI	1.64	3.82	$4s^2\,^2D$	$4p\,^2P^0$
46	609.59	1.52	1.33	InII	13.44	15.47	$5s6p\,^3P^0$	$5s6d\,^3D$

are most characteristic of this spectrum section. The presence of intense bands of a nitrogen molecule of the $C^3\Pi_u^+$–$B^3\Pi_g^+$ system and the spectral line 427.99 nm Cu II testify that, besides "escaping" electrons, the low-energy section of the electron energy distribution function also contains electrons with energies in the interval 9–18 eV, which are responsible for the emission by a nitrogen molecule in the spectral interval 290–410 nm. At the same time, the radiation emitted by indium atoms and singly charged ions in the visible spectral interval is represented by the spectral lines 410.17 nm In I, 451.13 nm In I, 462.07 nm In II, and 609 nm In II. The plasma emission spectrum also revealed a characteristic spectral line at a wavelength of 500.5 nm N II, which is often observed in the emission spectra of nanosecond discharges in atmospheric-pressure air [17, 18]. In the yellow-red section of the plasma radiation spectrum (Fig. 4), a low-intensity continuum was registered. The latter played a role of background for some low-intense spectral lines and molecular bands, which can be associated with the emission by selenium molecules.

As the nitrogen pressure was increased to 101 kPa and, accordingly, the value of the parameter E/N decreased by about twenty times (from about $1.5 \times \times 10^4$ V/(cm × mm Hg)), the character of the radiation spectrum of the nanosecond overvoltage discharge plasma changed (Fig. 4, *b*). This effect is possible provided that the efficiency of the ectonic mechanism of chalcopyrite electrode sputtering in a weaker electric field becomes lower and the mechanism of electrode sputtering under the impacts of positively charged nitrogen ions N^+ and N_2^+ (in the excited states, they manifest themselves in the radiation spectrum of discharge plasma; see Fig. 4, *b*) becomes switched on. In this case, the threshold of electron escape is not reached in the discharge [8], the electron distribution function over the energy changes, and the processes of energy transfer from nitrogen atoms and molecules in metastable states to chalcopyrite molecules or the products of their decay in plasma become more probable.

The main features in the emission spectrum of discharge plasma based on a nitrogen–$CuInSe_2$ vapor-gas mixture at $p(N_2) = 101$ kPa are associated with a significant intensity increase for the group of spectral lines Cu I, Cu II, and In II in a wavelength interval 200–250 nm, as well as with a reduction of their number. At the same time, the intensities

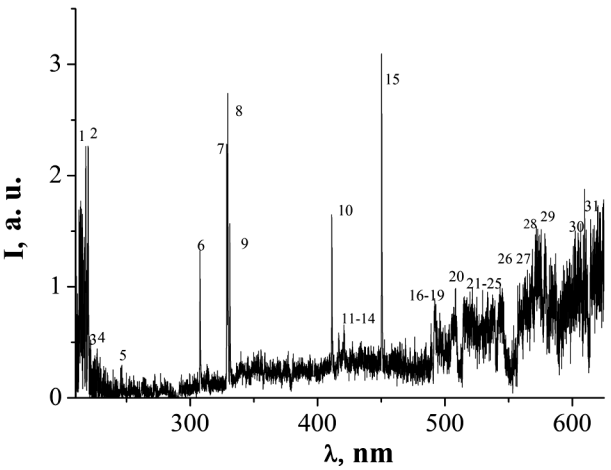

Fig. 5. Radiation emission spectra of nanosecond overvoltage discharge plasma between chalcopyrite electrodes at $p(\mathrm{Ar}) =$ 101 kPa

of the bands emitted by a nitrogen molecule drastically decrease. Instead of bands emitted by a nitrogen molecule in a spectral interval 290–460 nm, only separate intensive spectral lines Cu I, In I, and In II (lines 15 to 39) are observed in the radiation spectrum. The radiation emission in a spectral interval 550–630 nm had the form of molecular bands that played a role of the background for separate low-intensity spectral lines of atoms or ions. An accurate identification of this spectral interval requires the application of a spectrophotometer with a higher spectral resolution.

Figure 5 demonstrates the radiation spectrum of the nanosecond overvoltage discharge plasma ignited between chalcopyrite electrodes in the argon atmosphere at a pressure of 101 kPa. Table 2 illustrates the identification results for the most intense spectral lines and molecular bands, as well as their relative radiation intensities, in the spectrum exhibited in Fig. 5 and in an analogous spectrum registered at $p(\mathrm{Ar}) = 202$ kPa.

The radiation spectrum of the discharge plasma on the basis of an argon vapor-gas mixture in the spectral interval 200–250 nm included the same spectral lines – preferably, of the indium atom and the singly charged indium ion – as for the nitrogen-based plasma (Table 1). The increase of the argon pressure from 101 to 202 kPa gave rise to a substantial decrease in the radiation intensity of the spectral lines at 218.17 and 219.95 nm emitted by a copper atom. This reduction might occur owing to the growth of the UV radiation

Table 2. **Identification of the most intense spectral lines and bands of the products of the chalcopyrite molecule decomposition in the overvoltage nanosecond discharge at p(Ar) = 101 and 202 kPa**

No.	λ, nm	I, rel. units (at p(Ar) = 101 kPa)	I, rel. units (at p(Ar) = 202 kPa)	Object	E_{low}, eV	E_{up}, eV	Lower term	Upper term
1	218.17	2.26	0.33	CuI	0.00	5.68	$4s\,^2S$	$4p'\,^2P^0$
2	219.95	2.26	0.37	CuI	1.39	7.02	$4s^2\,^2D$	$4p''\,^2D^0$
3	225.57	0.34	1.66	InII	12.68	18.17	$5s5d\,^3D_3$	$5s4f\,^3F^0$
4	226.37	0.4	1.64	CuII	8.92	14.39	$4p'\,^1F^0$	$4d\,^3G$
5	246.02	0.3	0.41	InII	12.68	17.72	$5s5d\,^3D$	$5s7f\,^3F^0$
6	307.38	1.32	1.70	CuI	1.39	5.42	$4s^2\,^2D$	$4p'\,^2F^0$
7	328.27	2.13	2.35	CuI	5.15	8.93	$4p'\,^4F^0$	$4d'\,^2G$
8	329.05	2.74	3.27	CuI	5.07	8.84	$4p'\,^4F^0$	$4d'\,^4F$
9	330.79	1.56	1.76	CuI	5.07	8.82	$4p'\,^4F^0$	$4d'\,^4G$
10	410.17	1.65	1.75	InI	–	3.02	$5s^25p\,^2P^0$	$5s^26s\,^2S_{1/2}$
11	417.83	0.58	0.73	ArII	16.64	19.61	$4s\,^4P$	$4p\,^4D^0$
12	422.26	0.57	0.85	ArII	19.87	22.80	$4p\,^2P^0$	$5s\,^2P$
13	427.75	0.50	0.7	ArII	18.45	21.35	$4s'\,^2D$	$4p'\,^2P^0$
14	436.20	0.32	0.95	ArII	18.66	21.50	$3d\,^2D$	$4p'\,^2D^0$
15	451.13	3.1	3.27	InI	0.27	3.02	$5s^25p\,^2P^0$	$5s^26s\,^2S_{1/2}$
16	487.98	0.36	1.12	ArII	17.14	19.68	$4s\,^2P$	$4p\,^2D^0$
17	501.76	0.38	0.83	ArII	17.14	19.64	$4s\,^2P$	$4p\,^4D^0$
18	502.82	0.98	0.75	CuII	14.43	16.87	$4d\,^3D$	$4f\,^3F^0$
19	506.06	0.72	0.8	CuII	8.54	10.99	$4p\,^3P^0$	$4s^2\,^3P$
20	507.22	0.73	0.63	CuII	14.42	16.87	$4d\,^3F$	$4f\,^3F^0$
21	510.00	0.40	0.52	CuII	14.43	16.86	$4d\,^3D$	$4f\,^3D^0$
22	515.32	0.85	0.7	CuI	3.79	6.19	$4p\,^2P^0$	$4d\,^2D$
23	520.09	0.40	0.76	CuI	5.42	7.80	$4p'\,^2F^0$	$5s'\,^4D$
24	521.82	0.85	0.87	CuI	3.82	6.19	$4p\,^2P^0$	$4d\,^2D$
25	522.00	0.80	0.85	CuI	3.82	6.19	$4p\,^2P^0$	$4d\,^2D$
26	556.69	0.47	1.21	SeII				
27	557.69	0.7	0.90	InII	15.81	18.03	$5s7p\,^1P^0$	$5s10d\,^3D$
28	570.02	0.96	0.67	CuI	1.64	3.82	$4s^2\,^2D$	$4p\,^2P^0$
29	572.18	1.41	1.15	InII	15.29	17.46	$5s7s\,^1S$	$5s9p\,^1P^0$
30	594.92	1.02	1.10	ArI	13.28	15.35	$4p'[1\frac{1}{2}]$	$6d[1\frac{1}{2}]$
31	622.42	1.20	2.20	InII	15.77	17.76	$5s7p\,^3P^0$	$5s9d\,^3D$

absorption and to the increase in the partial pressure of the vapor of chalcopyrite and the products of its destruction in a discharge, because the pulse energy contribution to the discharge plasma increases under those conditions. In particular, for the spectral line 218.17 nm Cu I, the lower energy level is ground for the copper atom, so that the manifestation of self-absorption is typical of it. On the other hand, the intensities of the spectral lines of an indium ion mainly increased with the partial argon pressure and the energy contribution to the plasma (Table 2), as well as the intensities of lines of copper ion for the discharge between copper electrodes in atmospheric-pressure air [14, 15].

The second group of spectral lines (lines 6 to 15 in Table 2) was observed against a low-intensity continuous radiation background. The intensity of the latter weakly increased together with the wavelength (Fig. 5). The intensities of those spectral lines belonging to copper and indium atoms, as well as singly charged argon ions, increased with the argon pressure, the pulse energy contribution to the plasma,

and, hence, the vapor density of chalcopyrite and the products of its decay in the discharge. The radiation spectrum in the spectral interval 460–630 nm had the form of molecular bands playing the role of a background for separate low-intensity spectral lines of atoms and ions. Most probably, the emission spectrum of the discharge plasma in this spectral interval is a result of the radiation emission by selenium molecules, as well as argon atoms and ions. In order to diagnose the process of sputtering of chalcopyrite thin films onto solid glass or quartz substrates, the following intense spectral lines of copper and indium atoms in the spectral interval 300–460 nm can be used: 307.38 nm Cu I, 329.05 nm Cu I, 410.17 nm In I, and 451.13 nm In I.

4. Numerical Simulation of Plasma Parameters

Numerical calculations of the parameters of the plasma concerned were performed under an assumption that the chalcopyrite molecule can be substituted by a copper atom. The latter governs the main emission characteristics of the discharge and is the least strongly bound one in a chalcopyrite molecule. This is associated with the absence of information on effective cross-sections for the electron interaction with a $CuInSe_2$ molecule. The concentration of a copper vapor for the simulation was selected on the basis of data of work [19], where the copper vapor was created in the discharge gap by evaporating electrodes. As a result, there emerged traces of erosion at the working surface of electrodes in the form of separated zones up to 100–200 μm in diameter. They were identical to those obtained in our present experiment at a repetition frequency of 100 Hz for discharge pulses.

The maximum value of the E/P parameter in our experiments (at the nitrogen pressure $p = 101$ kPa and the discharge gap $d = 10^{-3}$ m) was about 530 V/(cm Torr) and, according to the local criterion of switching on the mode of continuous electron acceleration ("escape"), did not exceed the critical value of this parameter for nitrogen, 590 V/(cm Torr) [20]. Recent results of numerical simulation of the electron "escape" in the atmospheric-pressure nitrogen plasma showed that this threshold is much higher, reaching a value of 4000 V/(cm Torr) [21]. Proceeding from this fact, a standard computer program aimed at the solution of the stationary Boltzmann kinetic equation in the two-term approximation for the electron energy distribution function (EEDF) was chosen for the numerical modeling of parameters of the atmospheric-pressure nitrogen plasma with small admixtures of chalcopyrite vapor. The parameters of the discharge plasma in a mixture of nitrogen and copper vapor at a ratio between their partial pressures of 101 kPa : 30 Pa were calculated numerically as complete integrals of the EEDF. The EEDFs were determined by solving the Boltzmann kinetic equation in the two-term approximation. The EEDFs were calculated, by using a computer program [22], whose database for effective cross-sections also included information about the cross-sections of the electron interaction with copper atoms and nitrogen molecules.

On the basis of the calculated EEDFs, the main plasma parameters and their dependences on the magnitude of the reduced electric field (i.e. the ratio between the electric field strength E and the total concentration N of nitrogen molecules and a small fraction of copper vapor) were determined. The parameter E/N was varied within the interval from 1 to 1000 Td (from 1×10^{-17} to 1×10^{-14} V cm^2), which included the values that were realized experimentally. In the integral of electron collisions with molecules and atoms, the following processes were taken into consideration: elastic scattering of electrons by copper atoms and nitrogen molecules, excitation of energy levels of copper atoms (threshold energies of 1.500, 3.800,and 5.100 eV, respectively), ionization of copper atoms (a threshold energy of 7.724 eV), excitation of energy levels of a nitrogen molecule: rotational levels (a threshold energy of 0.020 eV), vibrational levels (threshold energies of 0.290, 0.291, 0.590, 0.880, 1.170, 1.470, 1.760, 2.060, and 2.350 eV), electron levels (threshold energies of 6.170, 7.000, 7.350, 7.360, 7.800, 8.160, 8.400, 8.550, 8.890, 11,03, 11.87, 12.25, and 13.00 eV), ionization (a threshold energy of 15.60 eV). The average electron energy in the discharge excited in the nitrogen-copper vapor-gas mixture (101 kPa : 30 Pa, ($E = 1.5 \times 10^7$ V/m, $E/N = 615$ Td) reached a value of 2.306 eV from 50 ns after the voltage pulse began till the time moment $t = 280$ ns. From the time moment $t = 280$ ns to the voltage pulse end ($t = 500$ ns) at $E = 0.75 \times 10^7$ V/m and $E/N = 307$ Td, the average energy of the discharge electrons amounted to 0.887 eV. The results of numerical calculations of the main plasma discharge parameters are quoted in Tables 3 and 4.

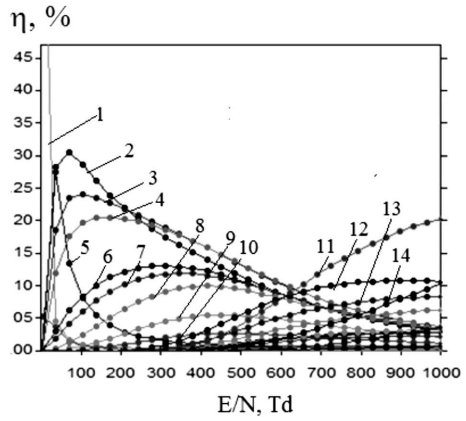

Fig. 6. Dependences of the specific losses of discharge power at electron collisions with nitrogen molecules on the parameter E/N in plasma with partial pressures Cu : N_2 = = 30.3 Pa : 101 kPa at the total pressure P = 101.030 kPa. Panel *a*: excitation of rotational level N_2 (*1*), excitation of vibrational level N_2(V = 1 res.) (*2*), excitation of vibrational level N_2(V = 2) (*3*), excitation of vibrational level N_2(V = 3) (*4*), excitation of vibrational level N_2(V = 1) (*5*), excitation of vibrational level N_2(V = 4) (*6*), excitation of vibrational level N_2(V = 5) (*7*), excitation of vibrational level N_2(V = 6) (*8*), excitation of vibrational level N_2(V = 7) (*9*), excitation of vibrational level N_2(V = 8) (*10*); panel *b*: excitation of electron state N_2(C3) (*11*), excitation of electron state N_2(B3) (*12*), excitation of electron state N_2(W3) (*13*), summation over N_2 singlet states (*14*), excitation of electron state N_2(A3 V = 0–4) (*15*), excitation of electron state N_2(B′3) (*16*), excitation electron state N_2(A3 V = 5–9) (*17*), excitation of electronic state N_2(C3) (*18*), N_2 ionization (*19*)

Table 3. **Transport characteristics of electrons in a discharge in a mixture of nitrogen and copper vapor at their pressure ratio of 101 kPa : 30 Pa**

E/N, Td	ε, eV	T^0, K	V, m/s	N, cm^{-3}
615	2.306	26749.6	9.6×10^5	4.95×10^{19}
307	0.887	10289.2	7.0×10^5	5.89×10^{19}

The numerical simulation of electron transport characteristics in the discharge ignited in the mixture of nitrogen with copper vapor at their partial pressure ratio of 101 kPa : 30 Pa (see Table 1) showed that the growth of the reduced electric field strength E/N within the experimental interval gave rise to the increase of the average energy ε and the temperature T of electrons, as well as their drift velocity V in the electric field. On the contrary, the electron concentration N decreased at higher values of the reduced electric field strength. The rate constants of excitation and ionization of a copper atom and a nitrogen molecule by electrons also increased with the parameter E/N (see Table 2). The corresponding maximum values were observed for the excitation constant of the resonance level of a copper atom.

Specific losses of the discharge power in an N_2–Cu gas-vapor mixture at a component pressure ratio of 101 kPa : 30 Pa, which were spent on the inelastic processes of electron collisions with mixture components, were maximum for nitrogen molecules (Fig. 6). They amounted to about 30% for the vibrational excitation of a nitrogen molecule N_2 and reached a maximum at a reduced electric field strength of 104 Td. For copper atoms, they did not exceed 0.8% (achieved for the excitation of the resonance state $2P_{3/2,1/2}$ of a copper atom at E/N = 724 Td). For a reduced electric field strength of 615 Td, the specific discharge power losses were about 0.7%. When the parameter E/N increased to 1000 Td, the specific discharge power losses in this gas-vapor mixture reached a maximum of 20.3% for the electron excitation of the electron state N_2(C3).

The values, as well as the growth and recession rates, of discharge power losses spent on the processes of electron state excitation and ionization are governed by the magnitudes of the effective cross-sections of inelastic electron collisions with the components of the working environment and their dependences on the electron energy, as well as by the dependence of the electron energy distribution function on the reduced electric field strength and by the threshold energy of the process. The specific discharge power losses for the excitation and ionization of a copper atom are low because of the low content of copper vapor in the mixture.

Therefore, according to the obtained distribution of discharge power losses for electronic processes, one may expect a significant role of the energy transfer processes from metastable nitrogen molecules to copper atoms in the plasma concerned. This assumption was experimentally confirmed, when studying the dynamics of radiation emission of a subnanosecond discharge plasma ignited between copper electrodes in the nitrogen atmosphere with the ectonic mechanism of copper vapor insertion into plasma [23]. In the cited experiments, the long (for about 2 ms) afterglow of a copper atom was detected, which exceeded

Table 4. **Rate constants of electron excitation (k) and ionization (k_i) of resonance (k_r) and metastable (k_m) levels of copper atom and nitrogen molecule in plasma on the basis of a mixture of nitrogen (101 kPa) and copper vapor (30 Pa)**

E/N, Td	$k_r \times 10^{+13}$, m^3/s	$k_m \times 10^{+14}$, m^3/s	$k_i \times 10^{+14}$, m^3/s	$k_r \times 10^{+16}$, m^3/s	$k_m \times 10^{+17}$, m^3/s	$k_i \times 10^{+17}$, m^3/s
	Cu			N_2		
615	0.63	0.49	0.11	0.29	0.78	0.28
307	0.02	0.025	0.002	0.0052	0.02	0.000093

the duration of a current pulse by three orders of magnitude.

5. Radiation Transmission Spectra of Chalcopyrite Films

In the spectral interval 200–300 nm, the absorption coefficient of thin films based on the $CuInSe_2$ compound decreased from 6×10^5 to 4×10^5 cm^{-1} and remained almost constant (4×10^5 cm^{-1}) in the wavelength interval 300–400 nm [1]. As the wavelength increased further from 400 to 1000 nm, the absorption coefficient decreased to 10^4 cm^{-1}, and, in the spectral interval 1000–1200 nm, it decreased exponentially to a value of 10 cm^{-1}. As follows from those results, the coefficient of light absorption in chalcopyrite films is large and strongly depends on the incident radiation wavelength.

Let us consider the relative light transmission spectra in the ultraviolet and visible spectral intervals for thin chalcopyrite films that were synthesized with the help of nanosecond overvoltage discharges in the nitrogen, argon, and air atmospheres. Typical transmission spectra for thin films based on the $CuInSe_2$ compound in the spectral interval 200–800 nm measured at various pressures in the oxygen-free gas medium (e.g., nitrogen) and at the atmospheric pressure in air are shown in Fig. 7. The transmission spectra for films synthesized in argon were similar.

The transmittance of thin chalcopyrite films, in comparison with that of the substrate, became about 2–2.5 times lower, and, for the film synthesized using a discharge in nitrogen, it was minimum at $p(N_2) =$ $= 101$ kPa. The forms of light transmission spectra for chalcopyrite films at nitrogen pressures of 13.3 and 101 kPa were close to each other. A lower transmittance of the film synthesized at $p(N_2) = 101$ kPa in comparison with that of the film synthesized at

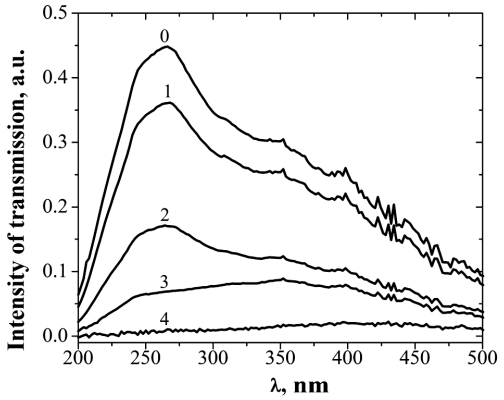

Fig. 7. Spectra of light transmission through chalcopyrite films sputtered on quartz substrates at their probing with deuterium lamp radiation: no specimen (*0*), pure quartz glass (*1*), $CuInSe_2$ electrodes at $p(N_2) = 13.3$ kPa (*2*), $CuInSe_2$ electrodes at $p(N_2) = 101$ kPa (*3*), $CuInSe_2$ electrodes in atmospheric-pressure air (*4*)

$p(N_2) = 5.5$ kPa can be associated with a smaller thickness of the film synthesized at the lower nitrogen pressure.

The lowest light transmittance of chalcopyrite films, which was an order of magnitude lower than that of a pure substrate, was obtained for specimens synthesized in atmospheric-pressure air. However, the presence of oxygen in a plasma can lead to its insertion into the film, which can affect the film characteristics. Strong absorption of the deuterium lamp radiation by chalcopyrite films in the spectral interval 200–500 nm takes place because, when thin chalcopyrite films are sputtered onto a substrate with the use of the gas-discharge method, and when electrodes based on the $CuInSe_2$ compound are applied, the films reproduce the stoichiometry of the electrode material. This is an important fact, if the synthesized films are intended to be used in photovoltaic devices.

After the deuterium discharge lamp was changed to an incandescent one, the transmission spectra of the same chalcopyrite films were analyzed in the spectral interval 400–800 nm. In this case, the main features in the transmission spectra of chalcopyrite films registered at various nitrogen and argon pressures, as well as at the atmospheric pressure of air, correlated with the results shown in Fig. 7. A comparison of the transmission spectra obtained with regard for the spectra of probe radiation and the transmission spectra of the substrate with the dependence of the absorption coefficient on the probe radiation wavelength demonstrated a qualitative correlation between them, which testifies that the composition of the films was stoichiometrically close to that of the electrode material.

6. Conclusions

To summarize, we have found found that a homogeneous nanosecond discharge can be ignited between the electrodes fabricated on the basis of $CuInSe_2$ compound and separated by a distance of 10^{-3} m in the nitrogen or argon atmosphere with a pressure of 5.3, 101, or 202 kPa. The discharge is characterized by a pulse electrical power of 5.5–10.5 MW and an energy supply of 0.35–0.44 J per pulse to the plasma. The analysis of spectral characteristics of a plasma based on N_2(Ar)–$CuInSe_2$ vapor-gas mixtures showed that the most intense are the spectral lines of a copper atom in the interval 200–250 nm and the spectral lines of an indium atom and copper and indium ions in a longer wavelength interval. The character of plasma radiation spectra makes it possible to assume the selective mechanisms of formation of excited atoms and ions of copper and indium in a plasma, which consist in transferring the energy from metastable argon and nitrogen atoms and molecules. On the basis of the measured relative intensities of spectral lines emitted by copper and indium atoms and ions, the temperature and electron density in the researched plasma can be evaluated. The following separately located and most intense lines in the spectral interval 300–460 nm can be used to diagnose the sputtering of chalcopyrite films in the real-time mode: 307.38 nm Cu I, 329.05 nm Cu I, 410.17 nm In I, and 451.13 nm In I. The research of the relative transmittance spectra of a probe radiation in the wavelength interval 200–800 nm by chalcopyrite films synthesized with the use of the pulsed gas discharge method in the nitrogen, argon, and air environments showed that the transmittance is the lowest for films synthesized at atmospheric pressures, which is promising for their application in photovoltaic devices.

1. G.F. Novikov, M.V. Gapanovich. Third-generation Cu-In-Ga-(S, Se)-based solar inverters. *Usp. Fiz. Nauk* **187**, 173 (2017) (in Russian).
2. A.K. Shuaibov, A.Y. Minya, M.P. Chuchman, A.A. Malinina, A.N. Malinin, T.Z. Gomoki, Ya.Ch. Kolozvari. Optical characteristics of overstressed nanosecond discharge in atmospheric-pressure air between chalcopyrite electrodes. *Plasma Res. Expr.* **1**, 015003 (2018).
3. G.A. Mesyats. Electron avalanche from metal. *Usp. Fiz. Nauk* **165**, 601 (1995) (in Russian).
4. O.K. Shuaibov, A.O. Malinina, O.M. Malinin. *New Gas-Discharge Methods for Obtaining Selective Ultraviolet and Visible Radiation and Synthesizing Nanostructures of Transition Metals* (Goverla, 2019) (in Ukrainian).
5. S.V. Avtaeva, O.S. Zhdanov, A.A. Pikulev, E.A. Sosnin, V.F. Tarasenko. *New Directions in Scientific Research and Application of Excilamps* (STT Publishing, 2013) (in Russian).
6. E.Kh. Baksht, V.F. Tarasenko, Yu.V. Shut'ko, V.V. Erofeev. Point-like pulse-periodic UV radiation source with a short duration. *Quant. Electron.* **42**, 153 (2012).
7. V.M. Holovey, K.P. Popovych, M.V. Prymak, M.M. Birov, V.M. Krasilinets, V.I. Sidey. X-ray induced optical absorption in $Li_2B_4O_7$ and $Li_2B_4O_7$:Cu single crystals and glasses. *Physica B* **450**, 34 (2014).
8. V.Yu. Kozhevnikov, A.V. Kozyrev, N.M. Dmitrieva. Theoretical 0-D simulation of a high-pressure subnanosecond gas discharge. *Izv. Vyssh. Ucheb. Zaved. Fiz.* **57**, 130 (2014) (in Russian).
9. R.V. Hrytsak, A.O. Malinina, O.J. Minya, O.K. Shuaibov, S.Y. Neymet. Characteristics of overstressed nanosecond discharge between electrodes from chalcopyrite in argon of atmospheric-pressure. In *Abstracts of the 19th International Young Scientists Conference on Applied Physics, Taras Shevchenko National University, Kyiv, Ukraine,* May 21–25 (2019), p. 37.
10. I.E. Kacher, A.K. Shuaibov, M.Yu. Rigan, A.I. Dashchenko. Optical diagnostics of laser evaporation of polycrystalline compound $CuInS_2$. *Teplofiz. Vys. Temp.* **40**, 880 (2002) (in Russian).
11. O.K. Shuaibov, M.P. Chuchman, L.L. Shimon, I.E. Kacher. Research of optical characteristics and parameters of laser plasma of $CuInS_2$ polycrystalline fusion mixture and its components. *Ukr. Fiz. Zh.* **48**, 223 (2003) (in Ukrainian).
12. A.K. Shuaibov, M.P. Chuchman, A.I. Dashchenko. Research of the radiation dynamics of erosive laser plasma of $CuInS_2$ polycrystal. *Pis'ma Zh. Tekhn. Fiz.* **29**, 23 (2003) (in Russian).
13. L. Geza, A. Shuaibov, Sz. Sandor, L. Elemer. Spectroscopic diagnostics of spark discharge plasma at atmospheric-pressure. *J. Chem. Eng.* **8**, 302 (2014).

14. A.K. Shuaibov, A.Y. Minya, A.A. Malinina, A.N. Malinin, V. V. Danilo, M.Yu. Sichka, I.V. Shevera. Synthesis of copper oxides nanostructures by an overstressed nanosecond discharge in atmospheric-pressure air between copper electrodes. *Am. J. Mech. Mater. Eng.* **2**, 8 (2018).
15. A.K. Shuaibov, A.I. Minya, Z.T. Gomoki, V.V. Danilo, P.V. Pinzenik. Characteristics of a high-current pulse discharge in air with ectonic mechanism of copper vapor injection into a discharge gap. *Surf. Eng. Appl. Electrochem.* **55**, 65 (2019).
16. A.K. Shuaibov, G.E. Laslov, A.I. Minya, Z.T. Gomoki. Characteristics and parameters of nanosecond air discharge plasma between chalcopyrite electrodes. *Techn. Phys. Lett.* **40**, 963 (2014).
17. R.M. Van der Horst, T. Verreycken, E.M. van Veldhuizen, P.J. Bruggerman. Time-resolved optical emission spectroscopy of nanosecond pulsed discharges in atmospheric-pressure N_2 and N_2/H_2O mixtures. *J. Phys. D* **45**, 345201 (2012).
18. D.Z. Pai, D.A. Lacoste, Ch.O. Laux. Nanosecond repetitively pulsed discharges in air at atmospheric-pressure – the spark regime. *Plasma Sourc. Sci. Technol.* **19**, 065015 (2010).
19. A.S. Pashchina, A.V. Efimov, V.F. Chinnov. Optical research of multicomponent capillary discharge plasma. Supersonic outflow mode. *Teplofiz. Vys. Temp.* **55**, 669 (2017) (in Russian).
20. V.F. Tarasenko, S.I. Yakovlenko. Electron runaway mechanism in dense gases and formation of powerful subnanosecond electron beams. *Usp. Fiz. Nauk* **174**, 953 (2004) (in Russian).
21. http:/www.bolsig.laplace.univ-tlse.fr.
22. M.I. Lomaev, D.V. Beloplotov, D.A. Sorokin, V.F. Tarasenko. Spectral and amplitude–time characteristics of radiation of plasma of a repetitively pulsed discharge initiated by runaway electrons. *Opt. Spectrosc.* **120**, 171 (2016).
23. A.O. Malinina, R.V. Gritsak, O.K. Shuaibov, O.Y. Minya, O.M. Malinin. Pulse-periodic source of synchronized fluxes of bactericidal UV radiation and chalcopyrite ($CuInSe_2$) clusters and nanoparticles. In *Proceedings of the 8th International Conference "Medical Physics: Current State, Problems, Paths of Development. Novel Technologies", Kyiv, Ukraine, September 26–27* (2019), p. 216 (in Ukrainian).

Received 13.08.19.
Translated from Ukrainian by O.I. Voitenko

О.К. Шуаібов, О.Й. Миня,
А.О. Малініна, Р.В. Грицак, О.М. Малінін

ХАРАКТЕРИСТИКИ ПЕРЕНАПРУЖЕНОГО НАНОСЕКУНДНОГО РОЗРЯДУ МІЖ ЕЛЕКТРОДАМИ З ХАЛЬКОПІРИТУ ($CuInSe_2$) В БЕЗКИСНЕВИХ ГАЗОВИХ СЕРЕДОВИЩАХ

Р е з ю м е

Приведено характеристики перенапруженого наносекундного разряду в аргоні і азоті між напівпровідниковими електродами на основі сполуки $CuInSe_2$ при тисках газів 5,3–101 кПа. Внаслідок розпорошення електродів пари халькопіриту потрапляють в плазму розряду і молекули $CuInSe_2$ частково руйнуються, а частково осаджуються у вигляді тонких плівок на твердих діелектричних підкладках, розміщених поблизу системи електродів з плазмою. Встановлено основні продукти розпаду молекули халькопіриту в перенапруженому наносекундному розряді, що знаходяться у збуджених та іонізованих станах, і які представлені атомами та однозарядними іонами міді та індію. Запропоновано спектральні лінії атомів і іонів міді та індію, які можуть бути використані для контролю за процесом напилення тонких плівок халькопіриту в режимі реального часу. Шляхом числового розв'язку кінетичного рівняння Больцмана для функції розподілу електронів за енергіями, розраховані температура і густина електронів в розряді, питомі втрати потужності розряду на основні електронні процеси і константи швидкості електронних процесів в залежності від величини параметра E/N для плазми паро-газових сумішей на основі азоту і халькопіриту. На кварцових підкладках газорозрядним методом синтезовані тонкі плівки халькопіриту, які в широкому спектральному діапазоні (200–800 нм) ефективно поглинали світло. Це відкриває перспективи їх застосування в фотовольтаїчних пристроях.